

Genetic randomization reveals functional relationships among morphologic and tissue-quality traits that contribute to bone strength and fragility

Karl J. Jepsen · Bin Hu · Steven M. Tommasini ·
Hayden-William Courtland · Christopher Price ·
Carl J. Terranova · Joseph H. Nadeau

Received: 24 January 2007 / Accepted: 9 March 2007 / Published online: 8 June 2007
© Springer Science+Business Media, LLC 2007

Abstract We examined femora from adult AXB/BXA recombinant inbred (RI) mouse strains to identify skeletal traits that are functionally related and to determine how functional interactions among these traits contribute to genetic variability in whole-bone stiffness, strength, and toughness. Randomization of A/J and C57BL/6J genomic regions resulted in each adult male and female RI strain building mechanically functional femora by assembling unique sets of morphologic and tissue-quality traits. A correlation analysis was conducted using the mean trait

values for each RI strain. A third of the 66 correlations examined were significant, indicating that many bone traits covaried or were functionally related. Path analysis revealed important functional interactions among bone slenderness, cortical thickness, and tissue mineral density. The path coefficients describing these functional relations were similar for both sexes. The causal relationship among these three traits suggested that cellular processes during growth simultaneously regulate bone slenderness, cortical thickness, and tissue mineral density so that the combination of traits is sufficiently stiff and strong to satisfy daily loading demands. A disadvantage of these functional interactions was that increases in tissue mineral density also deleteriously affected tissue ductility. Consequently, slender bones with high mineral density may be stiff and strong but they are also brittle. Thus, genetically randomized mouse strains revealed a basic biological paradigm that allows for flexibility in building bones that are functional for daily activities but that creates preferred sets of traits under extreme loading conditions. Genetic or environmental perturbations that alter these functional interactions during growth would be expected to lead to loss of function and suboptimal adult bone quality.

K. J. Jepsen · B. Hu · H.-W. Courtland · C. Price
Leni & Peter W. May Department of Orthopaedics,
Mount Sinai School of Medicine,
New York, New York, USA

S. M. Tommasini
Department of Biomedical Engineering,
City College of New York,
New York, New York, USA

C. J. Terranova
Department of Anatomy,
Touro College of Osteopathic Medicine,
230 W. 125th Street,
New York, New York, USA

J. H. Nadeau
Department of Genetics and the Center for Computational
Genomics and Systems Biology,
Case Western Reserve University School of Medicine,
Cleveland, Ohio, USA

K. J. Jepsen (✉)
Department of Orthopaedics,
Mount Sinai School of Medicine,
One Gustave L. Levy Place,
Box 1188,
New York, NY 10029, USA
e-mail: karl.jepsen@mssm.edu

Abbreviations

BW	= Body weight
Le	= Length
Max	= Maximum load
Stiff	= Stiffness
PYD	= Postyield deflection
Work	= Work-to-fracture
CtAr	= Cortical area
TtAr	= Total area

MaAr	= Marrow area
J	= Polar moment of inertia
CtTh	= Cortical thickness
RCA	= Relative cortical area
TMDn	= Tissue mineral density

Introduction

Bones serve many critical functions, including joint movement, ambulation, and vital organ protection. Facilitating these functionalities requires that bone be mechanically stiff, strong, and tough. Although most individuals build bones that are functional for daily activities, a large fraction of these individuals sustain fractures during extreme loading events such as intense physical exercise or falls (Cummings and Melton 2002; Milgrom et al. 1985). A major determinant of this fracture risk is bone size. Having slender bones (i.e., small width relative to length) has been associated with increased risk of fracture in children (Chan et al. 1984; Landin and Nilsson 1983), young adult athletes and military recruits (Beck et al. 2000; Crossley et al. 1999; Giladi et al. 1987; Milgrom et al. 1989), and the elderly (Albright et al. 1941; Duan et al. 1999, 2001; Gilsanz et al. 1995; Kiel et al. 2001). The reason why slender bones are functional for daily activities but perform poorly under extreme load conditions remains unclear. The increased fracture incidence has generally been attributed to the reduced load-carrying capacity of smaller structures (Beck et al. 1996; Milgrom et al. 1989). However, recent data indicated that slender bones are also accompanied by matrix-level variations that deleteriously affect tissue quality (Tommasini et al. 2005b). This suggests that there are important interactions between morphologic and tissue-quality traits that may contribute to this clinical problem.

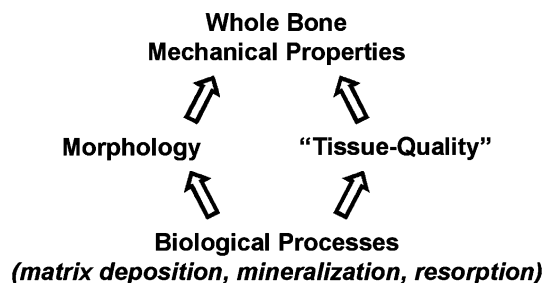
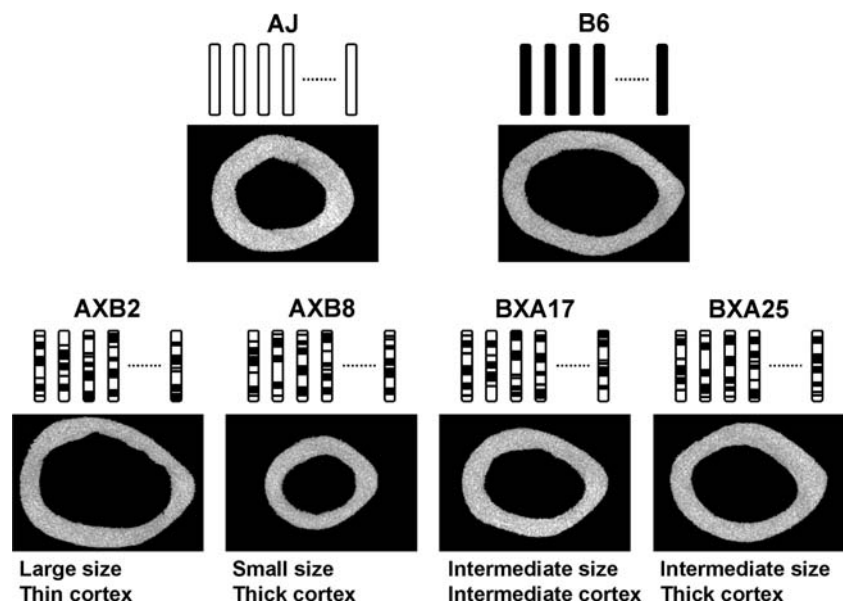


Fig. 1 According to engineering principles, whole-bone mechanical properties are determined by traits specifying bone size and shape (morphology) and traits specifying tissue-level mechanical properties (tissue quality). The physical bone traits are linked to genetic variation through variable cell behavior affecting the movement of bone surfaces and matrix deposition

Because most physical bone traits show a high degree of heritability (Leamy 1974; Susanne et al. 1983), novel strategies aimed at reducing fracture incidence may be developed by knowing how genetic variation affects the overall mechanical function of bone. Given our understanding of how mechanical function is achieved in bone (Fig. 1), at least two major issues need to be incorporated into genetic analyses. First, whole-bone mechanical function is defined by the joint contribution of traits specifying size and shape (i.e., morphology) and traits specifying tissue-level mechanical properties (i.e., tissue quality), the latter traits being defined by matrix composition and organization. Second, anecdotal evidence suggests that there are strong, biological processes that ensure the suite of morphologic and tissue-quality traits generates whole-bone mechanical properties that match daily loading demands (Currey 1979; Frost 1987; Olson and Miller 1958). Traits that covary to satisfy a common function are considered to be functionally related or functionally integrated (Cheverud 1996; Wright 1918). Although quantitative trait loci (QTLs) regulating complex properties like bone strength, fragility, and bone mineral density (BMD) have been identified (Beamer et al. 1999; Klein et al. 1998; Li et al. 2002a; Orwoll et al. 2001; Yershov et al. 2001), rarely have studies been conducted with knowledge of the relationships among genes, cellular processes, growth patterns, physical traits, and mechanical functions (Leamy et al. 1999; Li et al. 2002b; Li et al. 2006a; Mohan et al. 2003; Yershov et al. 2001). Because prior work focused primarily on morphologic integration (Leamy et al. 1999; Olson and Miller 1958; Wright 1918), the effects of variable tissue quality on organ-level function is unclear. Consequently, the identity of the traits that are functionally related and the manner in which these relationships define the repertoire of whole-bone stiffness, strength, and toughness are not fully understood.

Traditional reductionist approaches, because they relate individual bone traits with QTLs, are not useful for this level of analysis because they do not consider how the traits together define mechanical function. Rather, a systems approach is needed to test how variability in whole-bone mechanical properties arises when multiple physical bone traits (or gene sets) vary simultaneously. A viable option is to use path analysis, which is a powerful, multivariate method that analyzes covariances among traits, rather than mean values, in order to reveal functional relations among component traits within complex systems (Wright 1921). Path analysis has been used to study a variety of complex systems, including bone (Li et al. 2006a; Wright 1918) and rheumatoid arthritis (Li et al. 2006b). Because path analysis reveals how traits covary in the context of other traits within the system, this approach can be used to identify functional interactions among traits that would not be expected, especially for traits that are

Fig. 2 Representative mid-diaphyseal femoral cross sections obtained by micro-computed tomography show how the random segregation of genomic regions from A/J (white) and B6 (black) inbred mice leads to variability in bone morphology among the AXB/BXA RI strains. All sections were taken from female mice. Four AXB/BXA RI strains were chosen to illustrate the range in bone size and shape



defined by diverse sets of genes or biological processes. Importantly, the relationships determined within the multivariate system often differ from the relationships determined from bivariate regression analyses (Grace 2006). Thus, path analysis, because it provides an accurate representation of functional interactions and deterministic relationships among traits, can be used to understand how gene-level variation leads to increased risk of fragility fractures in bone (Li et al. 2006a).

The goals of this study were to identify bone traits that are functionally related and to determine how these functional interactions contribute to variability in whole-bone stiffness, strength, and toughness. We studied these interactions using inbred mouse strains because different strains show widely varying skeletal traits (Jepsen et al. 2003) and because transverse growth patterns of mouse long bone, which defines bone slenderness, are similar to human long bone (Garn 1970; Price et al. 2005). Importantly, because different inbred mouse strains build mechanically functional bones by assembling different sets of physical bone traits during growth (Jepsen et al. 2001, 2003; Tommasini et al. 2005a; Turner et al. 2000; Wergedal et al. 2005), inbred mouse strains provide a valuable model to study how interactions among traits define mechanical functionality. We examined two particular inbred mouse strains, A/J and C57BL/6J (B6), because a biomechanical analysis revealed that A/J mice have more slender femoral diaphyses but thicker cortices and higher mineralization when compared with B6 mice, which have wider femoral diaphyses but thinner cortices and lower mineralization (Jepsen et al. 2001). Surprisingly, femora from the two strains showed similar stiffness values, suggesting that there are interactions among bone size, cortical thickness,

and mineral density and that these interactions are important for building a functional bone. However, A/J femora failed in a more brittle manner compared with B6, indicating that these strains provide a valuable model to investigate why genetic variations that affect bone slenderness also affect bone fragility.

To test the hypothesis that bone size, cortical thickness, and mineral density are functionally related, we conducted a path analysis using data derived from a panel of AXB/BXA recombinant inbred (RI) mouse strains. RI strains have a unique pattern of genetic randomization that can be used to measure the tendency for different traits to cosegregate (i.e., correlate) in a natural, nonpathologic manner rather than to map genes (Nadeau et al. 2003). For long bones like the femur, each RI strain will show a unique suite of adult traits (Fig. 2), depending on how the particular set of genes for each strain influenced the cellular processes regulating bone growth (Price et al. 2005). Certain bone traits are postulated to covary so that organ-level functionality (i.e., adequate whole-bone stiffness) is achieved for each RI strain. Because the size, shape, and tissue quality of the femoral diaphyses will differ among the RI strains, a correlation analysis conducted across the RI panel should thus reveal which traits covary. If the interactions among bone size, cortical thickness, and mineral density are part of a basic biological paradigm that facilitates the development of organ-level functionality, then we would expect to see these particular traits covary across the RI panel. To test how the functional interactions among these bone traits define whole-bone mechanical properties, we conducted additional path analyses that included whole-bone stiffness and toughness and developed causal models based on engineering principles.

Methods

Recombinant inbred mouse strains

AXB/BXA RI mice derived from A/J and C57BL/6J (B6) progenitor strains were examined in this study. Male and female A/J, B6, and 20 AXB/BXA RI strains ($n = 9\text{--}17/\text{genotype/sex}$) were bred at The Jackson Laboratory (Bar Harbor, ME, USA) and shipped to the Mount Sinai School of Medicine (New York, NY, USA) at 3.5 weeks of age. Including males and females allowed us to test whether dimorphic bone growth patterns lead to sex-specific interactions among traits. The handling and treatment of mice was approved by the Institutional Animal Care and Use Committee. To standardize environmental conditions, mice were fed a standard rodent chow (Purina Rodent Chow 5001) and water *ad libitum*, subjected to a 12-h light:dark cycle, and raised with approximately 5 mice/cage in the same room. Mice were killed at 16 weeks of age because previous studies showed that growth-related changes in traits slowed prior to this age (Price et al. 2005). Femora were harvested and stored frozen in phosphate buffered saline at -20°C . Femoral length (Le) was measured from the proximal femoral head to the distal condyles using digital calipers (0.01-mm resolution).

Physical bone traits

Diaphyseal cross-sectional morphology and tissue mineral density (TMDn) of the femur were measured using an eXplore Locus SP Pre-Clinical Specimen MicroComputed Tomography system (GE Healthcare, London, Ontario, Canada). Three-dimensional images of the entire femur were obtained at an $8.7\text{-}\mu\text{m}$ voxel size. The analysis region was limited to a 2.5-mm region of the mid-diaphysis that was located immediately distal to the third trochanter (Fig. 3). This site corresponded to the location where most femora failed during the four-point bending tests (see below). Femora were individually thresholded using a standard thresholding algorithm (Otsu 1979) to segment bone and nonbone voxels. A custom analysis program (The Mathworks, Inc., Natick, MA, USA) was developed to quantify morphologic traits describing the amount of tissue (cortical area, CtAr; marrow area, MaAr; total area, TtAr; cortical thickness, CtTh) and the spatial distribution of tissue (moment of inertia, J). Moment of inertia is a measure of the proximity of the tissue to the geometric centroid of the cross section. The amount and distribution of tissue are both necessary to properly relate diaphyseal morphology to mechanical function, because bones having the same cross-sectional area but different moments of inertia (e.g., a solid cylinder and a tube) will exhibit different mechanical behaviors under bending and torsional loads (van der Meulen

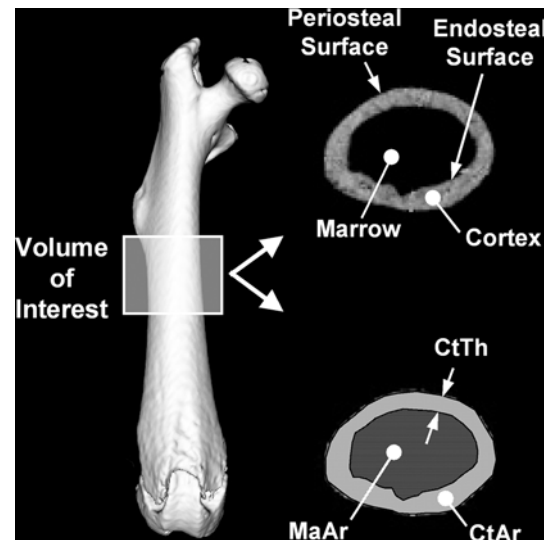


Fig. 3 Tomographic image of a mouse femur rendered in three dimensions shows the region of analysis and a representative mid-diaphyseal cross section. The periosteal and endosteal surfaces define the outer and inner (marrow) boundaries of the cortex, which is the mineralized structure that supports load

et al. 2001). Total bone area was defined as the sum of the cortical and marrow areas. The relative cortical area ($\text{RCA} = \text{CtAr}/\text{TtAr}$) provided a measure of the proportion of the total area that was occupied by bone. These traits were quantified for each cross section and the values were averaged over the volume of interest. The morphologic parameters measured by micro-computed tomography were found to be within 1% of histologically determined values for an independent set of adult AJ, B6, and C3H/HeJ femora (data not shown).

The microCT images were also used to quantify tissue mineral density (TMDn). TMDn is the average mineral value of the bone voxels only and was expressed in hydroxyapatite (HA) density equivalents. TMDn was calculated by converting the gray-scale output of bone voxels in Hounsfield units (HU) to mineral values (mg/cc of HA) through the use of a calibration phantom containing air, water, and HA (SB3: Gamex RMI, Middleton, WI, USA). TMDn was defined as the average bone voxel HU value divided by the average HU value of the HA phantom multiplied by 1130 mg/cc (HA physical density). The same calibration phantom was included in all scans to adjust mineral density measurements for the variability in X-ray attenuation inherent to independent scan sessions. Validation studies using 44 mouse femora showed that tissue mineral content correlated linearly ($p < 0.01$) with both ash weight/hydrated weight and ash weight/dry weight (data not shown).

Whole-bone mechanical properties

Following microCT analysis, femora were loaded to failure in four-point bending at 0.05 mm/sec using a servohy-

draulic materials test system (Instron Corp.; Canton, MA, USA) to assess whole-bone mechanical properties (Jepsen et al. 2003). Load deflection curves were analyzed for stiffness (the slope of the initial portion of the curve), maximum load (Max Load), postyield deflection (PYD), and work-to-failure (Work). PYD, which is a measure of ductility, was defined as the deflection at failure minus the deflection at yield. Yield was defined as a 10% reduction of secant stiffness (load range normalized for deflection range) relative to the initial (tangent) stiffness. Work, which is a measure of toughness, was defined as the area under the load deflection curve. Femora were tested at room temperature and kept moist with phosphate buffered saline during all tests.

Comparison of female and male bone traits

Bone traits for male and female AXB/BXA RI strains were compared using a two-way analysis of variance (ANOVA) to test whether mechanical properties and physical bone traits were inherited in a sex-specific manner, similar to prior studies (Orwoll et al. 2001). A direct comparison between sexes was facilitated by converting trait values to Z scores to minimize size effects. A Z score was calculated for each femur as

$$Z \text{ score}_i = (x_i - x_{\text{ref}}) / \text{SD}_{\text{ref}}$$

where x_i is the trait value for each mouse femur and x_{ref} and SD_{ref} are the mean and standard deviation, respectively, calculated using the average values for all 20 AXB/BXA RI strains. This z transformation standardizes the variables so each trait shows a mean of zero and a standard deviation of one. Female and male values were z -transformed separately so that the phenotype of a female mouse was compared with that of other females and the phenotype of a male mouse was compared to that of other males.

Cosegregation of traits across the RI panel

To test whether bone traits covary, Pearson correlation coefficients were calculated for all trait-trait comparisons. This analysis used the mean Z scores for each RI strain in the panel. The correlation matrix retained the magnitude and direction (positive, negative) of each correlation coefficient. Statistically significant correlations were identified by establishing a threshold correlation magnitude. The correlation threshold was determined using permutation tests (Churchill and Doerge 1994; Nadeau et al. 2003), which corrects for multiple comparisons and establishes the maximum correlation coefficient that arises when the bone traits are randomly arranged across the RI panel.

Path analysis

A path analysis was conducted using the mean Z scores of each RI strain to determine how functional interactions among bone traits contribute to variability in whole-bone mechanical properties. Causal models were constructed by specifying the directed path between select bone traits. Directed paths identify related traits and indicate the direction of the causal relationship between them. Three causal models were constructed in order of increasing complexity. The first causal model (Fig. 7) was constructed to test the hypothesis that variability in bone size (TtAr) was causally related to variability in CtTh and TMDn. Because the causal path between CtTh and TMDn is not known *a priori*, we tested paths going in both directions. Femur length (Le), which is correlated with body weight, was included to take body size into consideration and to determine how variability in cross-sectional size (TtAr) relative to length (i.e., slenderness) relates to CtTh and TMDn. Males and females were tested separately, rather than using sex as a categorical variable, to generate two independent sets of path coefficients.

The second causal model added two variables to test how the functional interactions defined in the first model contributed to whole-bone stiffness (Fig. 8). Stiffness, which is a measure of the amount of deflection a bone undergoes while loaded, was used in this model because most theories suggest that bone adapts to daily loading demands by adjusting physical traits to keep peak tissue-level strains (deformations) within a certain range (Frost 1987). An advantage of using the femoral diaphysis in this analysis is that the mechanical behavior of cylindrical structures is well characterized. Cortical area (CtAr) was selected as the second variable because engineering principles state that stiffness depends on a measure of bone size and a measure of tissue quality, which was already represented in the first model (i.e., TMDn). The causal paths in the second model flow from the physical bone traits toward stiffness, since mechanical properties are the outward manifestation of the underlying traits.

The third model (Fig. 9) added two complex mechanical properties (PYD and work) to the prior models. These two mechanical properties capture the failure process of bone and thus differentiate whether a bone fails in a brittle (low PYD and work) or ductile (large PYD and work) manner during extreme loading events such as an overload condition.

Path coefficients, which represent the magnitude of the direct and indirect relationships between traits, were calculated based on the hypothesized causal models and the variance/covariance matrices of the observed data. Structural equations were constructed using the path coefficients to specify the interconnected, causal relationships. Analy-

ses were run for males and females separately using the standardized (z -transformed) data (LISREL v. 8.8; Scientific Software International, Lincoln Park, IL, USA). Observed and model-implied covariance matrices were compared using maximum likelihood estimation and overall fit was determined by a chi-squared test. Unlike conventional null hypothesis testing, path analysis favors the *a priori*, theory-based model such that models are rejected only if the observed data and the expectations derived from the model do not match (i.e., if $p < 0.05$) (Grace 2006). Thus, chi-squared (χ^2) values with an associated p value greater than 0.05 means that the data are adequately fit by the model. The root mean square error of approximation (RMSEA), which takes the number of degrees of freedom of the model into consideration (MacCallum and Hong 1997; Stieger and Lind 1980), was also reported as an additional fit index. For RMSEA, $p < 0.05$ indicates close fit, $0.05 < p < 0.08$ indicates fair fit, and $p > 0.10$ indicates poor fit (MacCallum and Hong 1997).

Results

Variation in bone traits among AXB/BXA RI mouse strains

The mean trait values and the standard deviations for each AXB/BXA RI strain are shown in Table 1 (females) and Table 2 (males). The mean values were normally distributed across the RI panel for all bone traits ($p > 0.1$, Kolmogorov-Smirnov test). Representative femoral cross sections of female RI strains (Fig. 2) illustrate how the size of the femoral diaphyses ranged from being smaller than A/J to larger than B6. The male RI panel (not shown) showed the same variation as the females. The overall mean trait values, which were determined by averaging across the RI panel (bottom row in Tables 1 and 2), were intermediate between the A/J and B6 parental strains for all traits.

Sex differences in bone trait inheritance

Trait values for female and male RI strains were compared to test whether bone traits were inherited in a sex-specific manner. For all bone traits, female and male data correlated in a linear manner and the R^2 values for the linear regressions ranged from 0.65 to 0.87 ($p < 0.0001$ for all regressions). Figure 4 shows representative regressions for a morphologic trait (total bone area) and a complex mechanical property (postyield deflection). Male RI strains tended to be heavier than their female counterparts, as expected, and this translated into male mice showing larger morphologic traits compared with those of females. Despite the differences in body size, a comparison of the Z

scores between male and female RI strains showed significant effects due to genotype ($p < 0.0001$, 2-way ANOVA), but not to sex ($p > 0.9$, 2-way ANOVA). Thus, the data indicated that male and female AXB/BXA RI strains inherited bone traits in a similar manner.

Cosegregation of traits across the AXB/BXA RI panel

A correlation matrix was established to identify the traits that cosegregated (i.e., correlated) in a significant manner (Table 3A and B). For 20 AXB/BXA RI strains and 12 traits, the permutation test indicated that a correlation coefficient of 0.66 corresponded to a significance level of $p < 0.1$, a correlation coefficient of 0.69 corresponded to $p < 0.05$, and a correlation coefficient of 0.75 corresponded to $p < 0.01$. Plotting the mean traits across the AXB/BXA RI panel revealed that many traits cosegregated in a significant manner for males and females (Fig. 5). Of the 66 correlations analyzed, females showed 27 strong correlations ($r > 0.66$, $p < 0.1$) and 22 of these were considered significant ($r > 0.69$, $p < 0.05$) (Table 3A). Males showed 17 strong correlations ($r > 0.66$, $p < 0.1$) with 13 considered significant ($r > 0.69$, $p < 0.05$) (Table 3B). The average number of strong correlations per trait was 4.5 for females and 2.6 for males, indicating that bone traits were highly connected or interdependent. Networks depicting the significant trait interactions are shown in Fig. 6.

Many of the significant correlations were expected, such as those between body weight and stiffness, maximum load, cortical area, and cortical thickness. Likewise, those between stiffness and maximum load and those among the morphologic traits were consistent with engineering and mathematical principles. However, some observed correlations were unexpected. For example, the negative relationship between RCA and MaAr indicated that the proportion of total area occupied by bone varied with the size of the bone such that smaller bones tended to have proportionally thicker cortices. Furthermore, the positive correlation between CtTh and TMDn indicated that the increased cortical thickness of slender bones was accompanied by a larger amount of mineral packed into the tissue. This last relationship was significant for females but weaker for males.

Functional interactions among physical traits

The first path model (Fig. 7) had no available degrees of freedom to properly assess goodness of fit. However, because the endogenous (TMDn, CtTh) and exogenous (TtAr, Le) variables were connected directly, the structural equations were equivalent to equations derived by multiple regression analyses and could thus be evaluated based on R^2 values. The structural equations for TMDn and CtTh

Table 1 Phenotypes for 16-week-old female A/J, B6, and AXB/BXA RI mouse strains Data are presented as mean \pm standard deviation. Means for the RI mice are shown in the last row

	<i>n</i>	BW	Le	Stiff	Max	PYD	Work	CtAr	TtAr	MaAr	J	CtTh	RCA	TMDn
		(g)	(mm)	(N/mm)	(N)	(mm)	(N mm)	(mm ²)	(mm ²)	(mm ²)	(mm ⁴)	(mm)		(mg/cc)
A/J	15	18.9	14.6	140.5	22.3	0.21	13.1	0.64	1.09	0.5	0.16	0.19	0.59	1351
		1.7	0.3	25.6	2.6	0.11	5.2	0.05	0.07	0.04	0.02	0.01	0.02	28
B6	15	20.6	15.4	157	25.1	0.62	29.4	0.77	1.57	0.81	0.31	0.17	0.49	1271
		0.9	0.2	15.3	1.0	0.18	6.5	0.02	0.05	0.04	0.17	0.01	0.01	34
AXB1	10	20.3	15.5	141.4	22	0.58	26.1	0.72	1.45	0.73	0.26	0.18	0.50	1291
		1.0	0.2	14.8	0.9	0.1	2.1	0.02	0.06	0.04	0.02	0.01	0.01	34
AXB2	17	20.2	15	148.7	23.8	0.45	24.7	0.77	1.74	0.97	0.34	0.17	0.44	1274
		1.1	0.3	18.7	2.0	0.12	6.3	0.03	0.08	0.06	0.03	0.01	0.02	39
AXB4	12	15.8	13.6	113.7	18.2	0.23	10.4	0.54	1.14	0.59	0.16	0.14	0.48	1289
		1.3	0.3	21.2	2.6	1.1	2.7	0.05	0.07	0.03	0.02	0.01	0.02	28
AXB5	9	19.3	14.7	136.2	19.9	0.27	13.4	0.62	1.26	0.63	0.19	0.17	0.49	1312
		1.1	0.3	13	2.7	0.08	4.3	0.05	0.07	0.02	0.02	0.01	0.02	34
AXB6	10	24	16.1	178.5	29.5	0.29	26.9	0.81	1.57	0.77	0.31	0.19	0.51	1332
		1.8	0.4	20.1	2.8	0.13	11.8	0.06	0.11	0.05	0.05	0.01	0.01	22
AXB8	14	18.2	15.1	109.1	15.4	0.21	9.2	0.52	0.84	0.32	0.09	0.18	0.61	1305
		2.9	0.5	17.3	2.4	0.12	3.3	0.05	0.05	0.02	0.01	0.01	0.03	40
AXB10	9	21.4	15.2	157.1	25.5	0.41	23.1	0.75	1.48	0.73	0.28	0.18	0.51	1255
		1.6	0.5	29.7	2.6	0.15	6.1	0.06	0.09	0.05	0.04	0.01	0.02	39
AXB12	9	19.8	14.5	111.5	19.2	0.44	18.5	0.56	1.27	0.71	0.18	0.15	0.44	1272
		1.6	0.4	20.4	2.3	0.21	7.6	0.05	0.06	0.03	0.02	0.01	0.03	37
AXB13	15	18.8	15.1	139.6	19	0.24	11.7	0.56	1.03	0.47	0.14	0.17	0.55	1301
		1.4	0.3	15.7	1.7	0.11	3.0	0.05	0.04	0.03	0.01	0.01	0.02	55
AXB15	10	24.8	15.5	176.9	28.3	0.29	24.2	0.73	1.25	0.52	0.21	0.21	0.58	1358
		1.4	0.2	19.9	1.4	0.12	5.6	0.03	0.06	0.04	0.02	0.01	0.02	39
AXB18	10	18.7	14.7	115.5	18.6	0.32	13.1	0.56	1.08	0.52	0.15	0.16	0.52	1296
		2.8	0.8	19.7	2.7	0.11	4.0	0.06	0.11	0.05	0.03	0.01	0.02	37
AXB19	10	22.9	15	147	22.1	0.49	21.2	0.66	1.22	0.56	0.2	0.18	0.54	1326
		1.8	0.4	12.4	1.2	0.24	6.2	0.04	0.08	0.05	0.02	0.01	0.02	22
AXB20	12	15.9	14.2	102.4	16.8	0.29	12	0.51	1.01	0.5	0.13	0.15	0.50	1279
		2.7	0.8	29.9	3.5	0.12	4.6	0.07	0.13	0.06	0.03	0.02	0.03	33
AXB23	10	20.5	14.5	132.8	21.9	0.36	19.1	0.65	1.31	0.66	0.22	0.16	0.50	1295
		0.9	0.2	21.4	1.4	0.17	5.2	0.04	0.07	0.04	0.03	0.01	0.01	25
AXB24	10	19.8	14.8	125.3	20.3	0.45	26.6	0.65	1.11	0.47	0.17	0.19	0.58	1304
		0.6	0.3	24.4	2.3	0.31	13.1	0.03	0.04	0.02	0.01	0.01	0.01	20
BXA7	10	23.1	15.6	190.4	28.5	0.39	25.9	0.77	1.61	0.83	0.32	0.18	0.48	1301
		1.1	0.3	29.1	2.4	0.15	4.3	0.03	0.05	0.03	0.02	0.01	0.01	35
BXA14	10	23.3	16.3	155.5	22.7	0.3	19.4	0.75	1.47	0.72	0.27	0.19	0.51	1322
		1.8	0.2	19.5	2.5	0.14	10.2	0.02	0.08	0.06	0.02	0.01	0.02	24
BXA17	10	22.6	15.3	145.4	22.6	0.36	17.3	0.66	1.22	0.55	0.2	0.18	0.54	1348
		1.0	0.2	18.2	1.6	0.13	5.0	0.03	0.06	0.03	0.02	0.01	0.01	37
BXA25	10	24.1	15.4	187.3	29.1	0.32	23.2	0.77	1.36	0.59	0.25	0.2	0.57	1341
		1.7	0.2	27.6	2.6	0.15	6.8	0.04	0.08	0.05	0.03	0.01	0.02	30
BXA26	10	17.9	14.7	162.9	24.5	0.15	12.6	0.68	1.24	0.57	0.20	0.18	0.54	1307
		1.3	0.2	11.4	1.2	0.08	4.4	0.03	0.07	0.04	0.02	0.004	0.01	28
Mean		20.6	15.1	143.9	22.4	0.34	18.9	0.66	1.28	0.62	0.21	0.18	0.52	1305
SD		2.6	0.6	26.5	4.2	0.11	6.1	0.09	0.22	0.15	0.07	0.02	0.05	27

Table 2 Phenotypes for 16-week-old male A/J, B6, and AXB/BXA RI mouse strains Data are presented as mean \pm standard deviation. Means for the RI mice are shown in the last row

	<i>n</i>	BW	Le	Stiff	Max	PYD	Work	CtAr	TtAr	MaAr	J	CtTh	RCA	TMDn (mg/cc)
		(g)	(mm)	(N/mm)	(N)	(mm)	(N mm)	(mm ²)	(mm ²)	(mm ²)	(mm ⁴)	(mm)		
A/J	15	23.7	15.1	150.7	24.2	0.22	14.7	0.69	1.16	0.47	0.19	0.20	0.60	1366
		1.8	0.2	19.1	2.1	0.11	3.7	0.04	0.06	0.03	0.02	0.01	0.01	33
B6	15	27.8	15.8	148.3	25.9	0.69	33	0.86	1.77	0.91	0.4	0.18	0.48	1248
		1.1	0.2	23.4	3.0	0.21	7.6	0.07	0.10	0.04	0.06	0.01	0.02	44
AXB1	10	26	15.7	156.5	26.3	0.62	32.4	0.79	1.56	0.77	0.31	0.19	0.51	1278
		1.1	0.2	23	1.4	0.19	5.9	0.03	0.03	0.03	0.02	0.01	0.02	25
AXB2	17	24.6	15.5	145.9	24.9	0.48	28.7	0.82	1.87	1.04	0.4	0.17	0.44	1263
		1.9	0.4	22.7	3.4	0.13	5.9	0.09	0.15	0.07	0.07	0.02	0.02	37
AXB4	12	20.1	14.6	131	23.8	0.22	14.2	0.7	1.31	0.61	0.24	0.17	0.53	1306
		2.5	0.3	24.8	2.8	0.10	3.8	0.07	0.11	0.06	0.04	0.01	0.02	41
AXB5	9	23.9	15.2	146.7	20.4	0.3	14.8	0.67	1.34	0.67	0.22	0.18	0.50	1307
		1.1	0.2	7.0	1.4	0.11	4.6	0.04	0.06	0.04	0.02	0.01	0.01	29
AXB6	10	28	16.5	179.9	32.4	0.28	23.6	0.89	1.84	0.95	0.42	0.19	0.49	1291
		1.7	0.3	24.6	2.8	0.08	7.2	0.06	0.13	0.08	0.05	0.01	0.02	30
AXB8	14	22.3	15.7	118.6	16.9	0.21	10	0.55	0.93	0.38	0.12	0.18	0.59	1240
		2.9	0.4	17	2.2	0.08	2.8	0.05	0.08	0.04	0.02	0.01	0.02	17
AXB10	9	28.3	15.6	139	26.8	0.42	25.5	0.87	1.67	0.8	0.38	0.19	0.52	1264
		2.3	0.2	13.6	3.0	0.11	8.4	0.07	0.12	0.06	0.06	0.01	0.01	45
AXB12	9	22.5	14.9	133.8	21.4	0.4	18.8	0.62	1.4	0.78	0.22	0.15	0.44	1273
		1.8	0.3	26.9	2.8	0.17	5.4	0.04	0.07	0.05	0.02	0.01	0.02	33
AXB13	15	21.5	15.4	133.5	19.5	0.26	12.4	0.59	1.06	0.46	0.15	0.17	0.57	1322
		2.8	0.5	20.9	1.7	0.10	3.3	0.05	0.11	0.08	0.03	0.01	0.04	25
AXB15	10	31.3	16.1	160.8	28.5	0.39	29.1	0.8	1.43	0.63	0.27	0.21	0.56	1322
		1.0	0.2	26.8	2.3	0.1	5.8	0.03	0.05	0.03	0.02	0.01	0.01	25
AXB18	10	23.4	15.2	118.6	20.8	0.46	20.2	0.65	1.19	0.54	0.19	0.18	0.55	1295
		2.0	0.4	20.3	2.3	0.26	8.3	0.05	0.08	0.04	0.03	0.01	0.02	34
AXB19	10	29.5	15.9	176.8	27.6	0.38	22.9	0.85	1.49	0.64	0.31	0.21	0.57	1343
		1.5	0.2	22.7	3.2	0.11	6.1	0.07	0.12	0.07	0.05	0.01	0.02	44
AXB20	12	24.5	15.3	137.4	24.9	0.36	19.8	0.71	1.35	0.64	0.24	0.18	0.52	1298
		3.3	0.6	28	4.4	0.13	7.1	0.11	0.17	0.07	0.07	0.02	0.03	38
AXB23	10	25.1	14.9	126.6	22.9	0.47	23.5	0.69	1.38	0.69	0.25	0.17	0.5	1292
		1.8	0.2	23.4	1.4	0.2	7.9	0.05	0.08	0.05	0.03	0.01	0.02	55
AXB24	10	26.6	14.9	143.6	21.9	0.45	27.6	0.7	1.27	0.57	0.22	0.19	0.55	1298
		2.4	0.2	9.2	1.8	0.12	8.2	0.04	0.05	0.02	0.02	0.01	0.01	38
BXA7	10	29.1	15.9	203	31.1	0.38	26	0.9	1.87	0.98	0.44	0.18	0.48	1278
		1.4	0.3	37.3	2.7	0.04	3.7	0.07	0.12	0.06	0.07	0.01	0.01	27
BXA14	10	29.5	16.4	162	24.3	0.23	13.9	0.89	1.85	0.95	0.42	0.19	0.48	1286
		3	0.3	18.4	1.9	0.05	3.4	0.06	0.15	0.1	0.06	0.01	0.02	32
BXA17	10	26.1	15.4	159.5	25.3	0.32	19.1	0.77	1.36	0.6	0.27	0.19	0.56	1329
		2.3	0.3	23.4	3.1	0.06	4.1	0.07	0.10	0.05	0.04	0.01	0.02	36
BXA25	10	30.7	16.2	223.5	32.7	0.29	24.7	0.89	1.59	0.71	0.34	0.21	0.56	1327
		1.7	0.3	22.3	2.3	0.08	5.9	0.06	0.09	0.05	0.04	0.01	0.01	16
BXA26	10	23.5	15.3	189.6	29.2	0.22	17.8	0.84	1.55	0.72	0.33	0.19	0.54	1314
		1.8	0.4	22.9	2.8	0.05	3.9	0.06	0.09	0.07	0.04	0.01	0.03	49
Mean		25.8	15.5	154.3	25.1	0.36	21.2	0.76	1.47	0.71	0.29	0.19	0.52	1296
SD		3.2	0.5	28.3	4.3	0.11	6.2	0.11	0.27	0.17	0.09	0.02	0.04	26

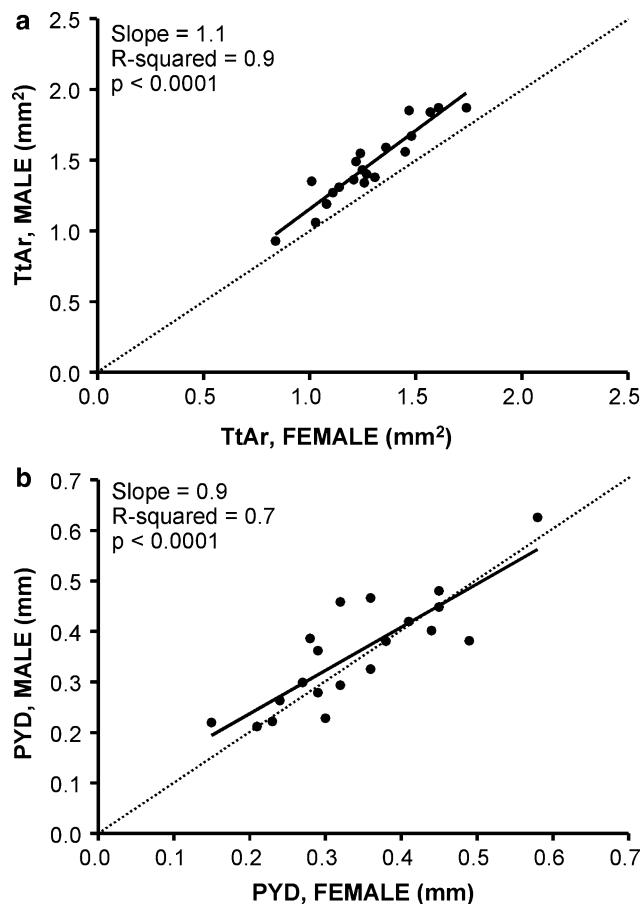


Fig. 4 Trait values for female AXB/BXA RI strains were regressed against the trait values of the corresponding male RI strain for (A) total area (TtAr) and (B) postyield deflection (PYD). The dashed line represents a perfect correlation with slope of 1

were significant ($p < 0.01$) and 45%-56% of the variability in TMDn and CtTh was explained by Le and TtAr for the male and female data sets. The path coefficients linking CtTh to Le and TtAr were similar for females and males, suggesting that variability in body size and bone cross-sectional size had similar effects on cortical thickness for both sexes. Importantly, the path coefficient between TtAr and CtTh was negative, indicating that a decrease in bone size (i.e., a more slender bone) was associated with a thicker cortex. The path coefficients for TMDn were also similar for females and males and indicated that CtTh and TtAr were significant predictors of TMDn. The structural equations indicated that when holding bone length fixed, a mouse showing a 1-SD decrease in TtAr (i.e., more slender bone) would also show an increase in CtTh by approximately 0.2 SD for females and males. Because TMDn was influenced by both TtAr and CtTh, the 1-SD reduction in TtAr would be associated with a 0.42-SD increase in TMDn for females $[-0.27$ (direct path) $+ -0.23 \times 0.67$ (indirect path) $= -0.42]$ and 0.34-SD increase in TMDn for

males $[-0.21$ (direct path) $+ -0.16 \times 0.79$ (indirect path) $= -0.34]$. Thus, the net effect of a unit change in TtAr on TMDn was similar for both sexes. These results indicated that mean trait values covaried among the RI strains in such a way that larger bones (i.e., larger outer diameter) tended to have thinner cortices and lower mineral content, whereas smaller bones (i.e., smaller outer diameter) tended to have thicker cortices and higher mineral content. Thus, the analysis of the RI panel indicated that there are important functional interactions among bone size (TtAr), cortical thickness (CtTh), and mineral density (TMDn).

Functional interactions contribute to bone stiffness

The second model (Fig. 8), which added CtAr and stiffness (Stiff) to the first model, showed a good fit for both males and females as determined by the χ^2 and RMSEA goodness-of-fit indices. Path coefficients were similar for both sexes, and 98% of the variation in cortical area (CtAr) was explained by TtAr and CtTh. The weak path coefficient for bone length indicated that length influenced CtAr indirectly through TtAr and CtTh. Stiffness was positively related to CtAr and TMDn for both females and males. The combination of a morphologic trait and a tissue-quality trait explained 70%-85% of the variation in stiffness for males and females.

Functional interactions contribute to bone fragility

In the third model (Fig. 9), adding PYD and work to the prior two models did not affect the goodness of fit as determined by χ^2 and RMSEA for either males or females. PYD was positively related to CtAr but negatively related to TMDn. These two traits explained 40% of the variation in PYD for females but only 20% for males. Work was positively related to both stiffness and PYD, and 88%-89% of the variation in work was explained by these two mechanical properties.

The robustness of Model C was tested by permuting directed paths and by substituting traits. For example, body weight was substituted for bone length, moment of inertia (J) was substituted for CtAr, marrow area (MaAr) was substituted for TtAr, and the direction of the path between CtTh and TMDn was reversed. These modifications had little effect on the goodness of fit or the variance explained by the structural equations. The only modifications that appreciably affected the model involved disrupting the path between CtTh and TMDn. Removing the path from CtTh to TMDn resulted in loss of goodness of fit for both males and females. This indicated that the functional interaction between CtTh and TMDn was important for explaining how variability arises in whole-bone mechanical properties.

Table 3 Correlation coefficients among bone traits for (a) female and (b) male AXB/BXA RI strains

	Stiff	Max	PYD	Work	CtAr	TtAr	MaAr	J	CtTh	RCA	TMDn
(A) Female											
Le	0.70	0.63	0.43	0.60	0.75	0.52	0.31	0.59	0.72	0.22	0.46
Stiff	xx	0.96	0.24	0.67	0.89	0.67	0.43	0.73	0.72	0.12	0.50
Max		xx	0.31	0.76	0.91	0.73	0.51	0.78	0.66	0.01	0.43
PYD			xx	0.79	0.56	0.58	0.52	0.59	0.27	0.18	0.10
Work				xx	0.86	0.75	0.57	0.79	0.59	0.05	0.21
CtAr					xx	0.87	0.67	0.92	0.65	0.08	0.31
TtAr						xx	0.95	0.99	0.21	0.56	0.06
MaAr							xx	0.90	-0.10	0.78	0.29
J								xx	0.31	0.45	0.00
CtTh									xx	0.67	0.70
RCA										xx	0.59
(B) Male											
Le	0.62	0.58	0.10	0.34	0.66	0.54	0.40	0.59	0.66	0.02	0.21
Stiff	xx	0.86	0.11	0.47	0.78	0.62	0.45	0.66	0.64	0.04	0.43
Max		xx	0.26	0.67	0.89	0.75	0.58	0.78	0.60	0.15	0.33
PYD			xx	0.85	0.36	0.39	0.37	0.37	0.15	0.27	0.20
Work				xx	0.65	0.59	0.48	0.59	0.44	0.19	0.03
CtAr					xx	0.90	0.73	0.94	0.62	0.25	0.16
TtAr						xx	0.96	0.99	0.24	0.65	0.12
MaAr							xx	0.91	0.02	0.83	0.29
J								xx	0.34	0.54	0.08
CtTh									xx	0.53	0.61
RCA										xx	0.51

Statistically significant correlations ($r > 0.69$, $p < 0.05$) are shown in bold

Discussion

Bone slenderness, cortical thickness, and mineral density are functionally related

The path analysis confirmed that the cross-sectional size of cortical bone, cortical thickness, and tissue mineral density were functionally related and determined that these functional interactions contributed to variability in whole-bone mechanical properties. Prior studies also reported correlations among bone traits (Ferretti et al. 1993; Jepsen et al. 2003; Tommasini et al. 2005a; Turner et al. 2000; Wergedal et al. 2005), but interpretations of these interactions were based largely on an intuitive sense of how bone works. Path analysis provides a rigorous, statistical method that explains how bone traits interact and how these interactions define complex mechanical properties. The covariation among traits observed in the RI panel indicated that the functional interactions among morphologic and tissue-quality traits are part of a basic biological paradigm that allows for flexibility in how organ-level functionality is achieved in mouse long bone. Thus, gene variants that affect bone slenderness may be accommodated by the

covariation of tissue quality and vice versa. The functional interactions observed in the path models also explain why certain traits and mechanical properties show pleiotropic effects (Yershov et al. 2001). The current data do not provide insight into whether variation in bone slenderness is causal to variation in mineral density or the opposite is true. The fact that the direction of the directed path between CtTh and TMDn had no effect on the model suggested that these traits covary with each other in a functional manner (i.e., are co-adapted).

Genetic randomization identified many functionally related traits

A principle finding of this study was that significant correlations were observed among many bone traits (22 for females and 13 for males) and that each trait was related to, on average, three to five other traits. These significant correlations support the hypothesis that many bone traits are functionally related and share common biological controls affecting growth (Wright 1918). In contrast to single-gene perturbations, which often create pathologic conditions (Bonadio et al. 1990) and in some cases elicit

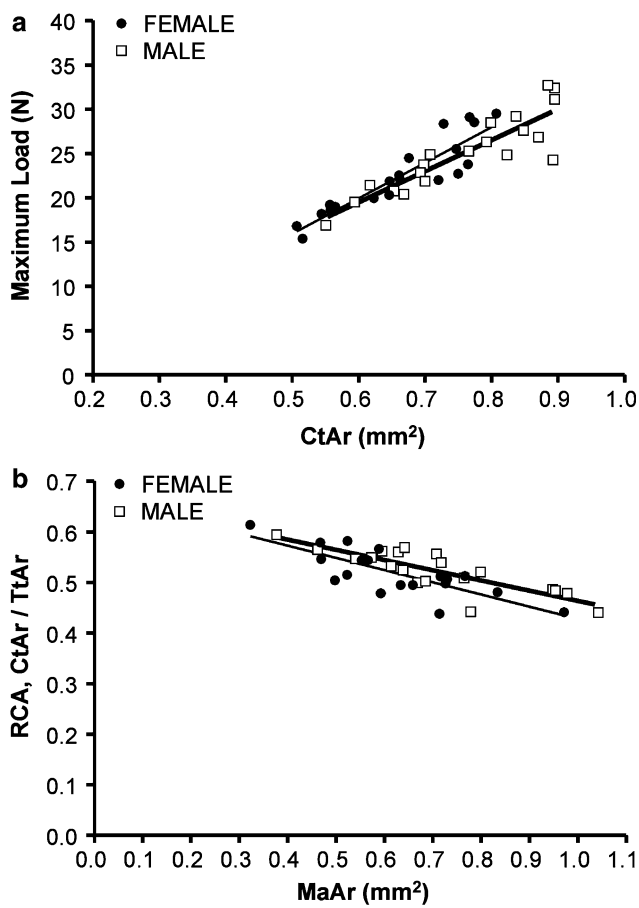


Fig. 5 Representative plots showing significant (a) positive (maximum load vs. cortical area) and (b) negative (relative cortical area vs. marrow area) correlations among bone traits for female and male RI strains. Individual data points represent the mean value for each AXB/BXA RI strain

strong, adaptive responses (Bonadio et al. 1993), this analysis used data derived from AXB/BXA RI strains to study how perturbing multiple genes simultaneously, in a nonpathologic manner, affected the construction of adult long bone (Nadeau et al. 2003). The results supported the premise that genetically randomizing genomic regions would result in each RI strain building a mechanically functional femur, but in slightly different ways, depending on the particular set of genes that were inherited from A/J and B6. None of the RI strains showed *in vivo* fractures, suggesting that each RI strain achieved organ-level functionality, i.e., a healthy bone. The randomization of A/J and B6 genomic regions was associated with a large range of trait values among the 20 AXB/BXA RI strains, and for several RI strains trait values exceeded (were larger or smaller) those of A/J and B6. This was expected given that these bone traits are genetically complex.

The correlations among stiffness, maximum load, PYD, and work-to-failure and those among stiffness and maximum load and the morphologic traits like CtAr and J were

expected because they are consistent with engineering principles (van der Meulen et al. 2001). The only major discrepancy between the current study and our prior work (Jepsen et al. 2003) was that the negative correlation between postyield deflection (PYD) and tissue mineral density was not statistically significant. Because tissue ductility has been shown to depend on mineral, collagen, and water content (Currey 1984; Martin and Ishida 1989; Wang et al. 2001), the weak correlation between PYD and TMDn highlights the need to expand the repertoire of matrix compositional traits to find more meaningful tissue-quality relationships. This is particularly important because small variations in TMDn are correlated with large changes in bone stiffness, strength, and ductility (Currey 1984).

Interactions among traits is critical for mechanical functionality

The path analysis provided an understanding of how variability in whole-bone mechanical properties arises from genetic variation in the underlying bone traits. The causal models, which were developed based on engineering principles and empirical data describing bone growth patterns (Price et al. 2005), showed good fits for both the male and the female data sets. The various trait substitutions and path additions/deletions had little effect on the model, suggesting that the relationships among traits fit the engineering-based causal models in a robust manner. The functional interactions among traits specifying cross-sectional bone size, cortical thickness, and mineralization indicated that more slender bones (smaller TtAr relative to length) were compensated by thicker cortices and higher tissue mineral density, whereas wider, more robust bones (larger TtAr relative to length) were compensated by thinner cortices and lower tissue mineral density. The fact that perturbing the interactions among these traits resulted in inadequate fits for the models suggested that the functional interaction between morphology and tissue quality was a fundamental biological process that allowed each RI strain to achieve an appropriate whole-bone stiffness during growth. Although the data do not reveal the details of the biological processes or the genes responsible for these functional interactions, the fact that the physical traits of each RI strain covaried in such a way that adult bones were sufficiently stiff and strong for loading demands suggested that these biological processes were adaptive in nature (Frost 1987).

The path analysis revealed novel interactions between traits that do not have an obvious relationship (e.g., TMDn and morphology). The positive correlation between cortical thickness and TMDn suggested that there is coordinate biological regulation between the amount of mineral packed into the matrix (TMDn) and the relative movements of the periosteal (TtAr) and endosteal (MaAr) surfaces that

Fig. 6 Network diagram shows traits that correlate significantly for females and males. Positive correlations are indicated by solid lines. Negative correlations are indicated by dashed lines

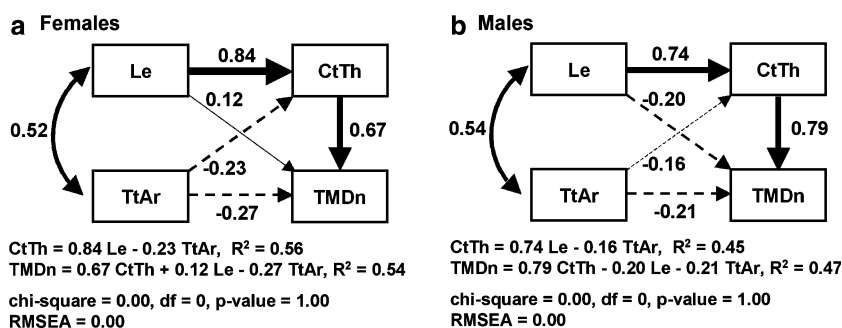
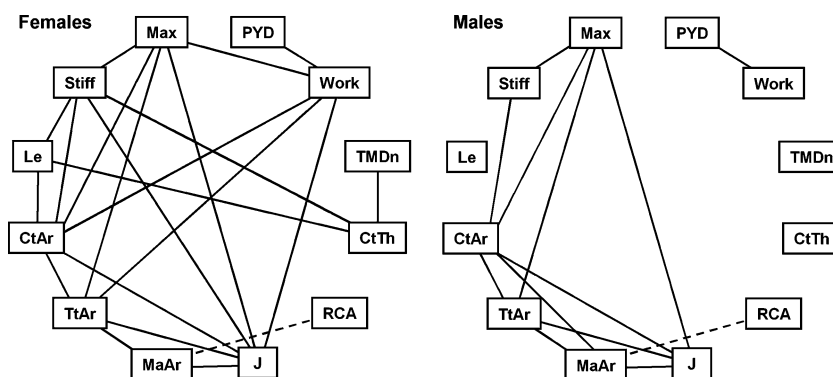


Fig. 7 Causal Model A was constructed to test for functional interactions among physical bone traits. Path diagrams for Model A show path coefficients between functionally related bone traits for (a) females and (b) males. Straight arrows indicate which traits are

related and the causal direction between them. Curved arrows indicate unresolved (noncausal) relationships. Structural equations and goodness-of-fit indices are shown below each path model

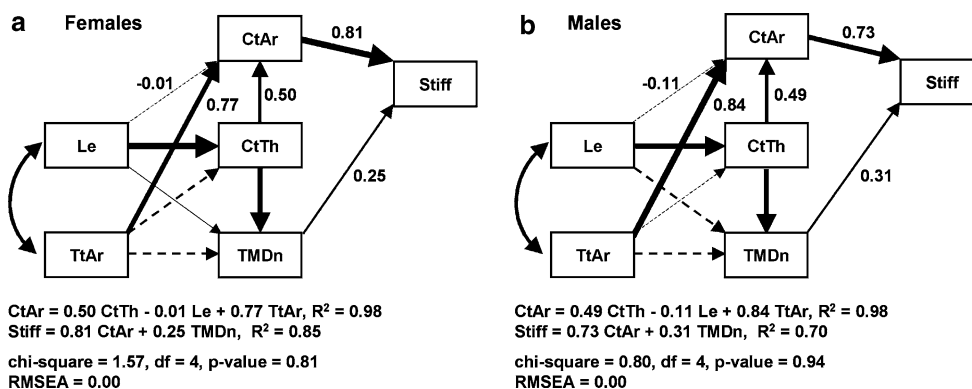


Fig. 8 Causal Model B was constructed to determine how interactions among the physical bone traits of Model A and a measure of bone size (CtAr) contribute to variability in whole-bone stiffness (Stiff). Path diagrams for Model B show path coefficients between functionally related bone traits for (a) females and (b) males. Path

coefficients are shown only for the added variables. Straight arrows indicate which traits are related and the causal direction between them. Curved arrows indicate unresolved (noncausal) relationships. Structural equations and goodness-of-fit indices are shown below each path model

define all morphologic traits, including cortical area, cortical thickness, and moment of inertia. A similar relationship between cortical thickness and mineral density was reported previously (Wergedal et al. 2005). Total area (TtAr) was treated as an exogenous (independent) variable in the causal models because this particular trait reflects the movement of the periosteal surface. Cortical thickness

provides a measure of the relative expansion of the endosteal surface, which defines the size of the marrow cavity (i.e., MaAr). These correlations argue strongly for a high degree of biological control over the final multivariate product. This coordinate regulation of traits is consistent with the concept of morphologic integration described five decades ago (Olson and Miller 1958). Although prior

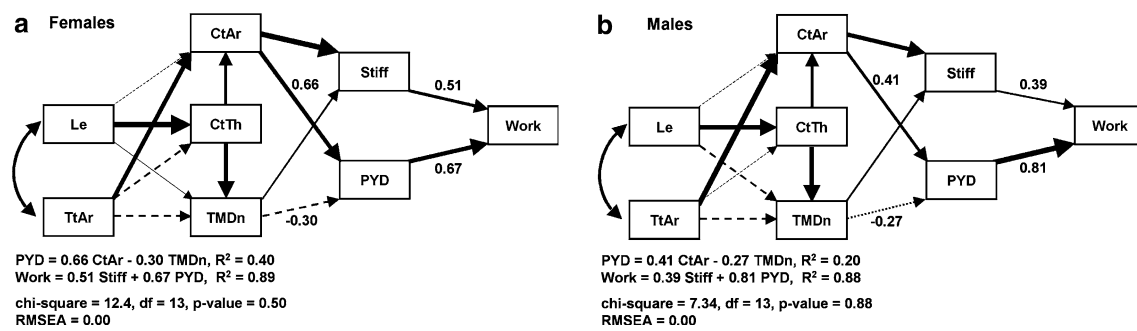


Fig. 9 Causal Model C was constructed to determine how interactions among physical bone traits contribute to variability in whole-bone ductility (PYD) and toughness (work-to-failure). Path diagrams for Model C show path coefficients between functionally related bone traits for (a) females and (b) males. Path coefficients are shown only

for the added variables. Straight arrows indicate which traits are related and the causal direction between them. Curved arrows indicate unresolved (noncausal) relationships. Structural equations and goodness-of-fit indices are shown below each path model

studies focused largely on the genetic and biological mechanisms regulating bone morphology (Leamy et al. 1999; Richman et al. 2001), the current data indicated that variation in bone morphology is also linked to variation in matrix composition and thus to tissue quality (Swartz et al. 1992). This analysis, which was conducted using a single bone from a single species, is consistent with prior comparative analyses that examined bones serving different functions from different species (Currey 1979). Thus, the interaction between bone morphology and tissue quality appears to be an important biological paradigm for bone. Further studies need to be conducted to determine if the functional interactions identified for AXB/BXA RI femora hold for different bones or for different intercrosses and outbred populations.

Although this study was conducted using genetically randomized mouse strains, there is no reason to expect that functional interactions are limited to multigenetic variation. If the functional interactions among traits are a basic biological paradigm, then environmental perturbations or single-gene mutations that alter cross-sectional bone size would be expected to also perturb tissue quality and vice versa. For example, a mutation affecting type I collagen synthesis was associated with reduced tissue strength and a compensatory age-related increase in bone size (Bonadio et al. 1993). Although the data do not reveal the limits to the amount of variation that can be accommodated by the underlying biological processes, the skeletal dysfunction associated with certain genetic mutations (e.g., osteogenesis imperfecta) and environmental perturbations (e.g., scurvy) clearly tell us that not all genetic or environmental variations can be accommodated by the functional interactions among bone traits. Understanding these limits and how to perturb the environment to facilitate a positive response may provide new targets for genetic analyses as well as new strategies for building more robust bones during growth.

Interactions among traits establishes preferred sets of traits

Although the trait sets for each RI strain appeared to achieve the appropriate stiffness and strength for day-to-day activities, not all sets of traits resulted in satisfactory values for PYD or work-to-failure (e.g., AXB5, AXB13, BXA26). These latter mechanical properties are important because they reflect the failure process of bone. Brittle failures are associated with low values for PYD and work-to-failure. A brittle femur would be expected to perform poorly under extreme loading conditions such as the cyclic loading associated with intense physical exercise or the high-impact loads associated with falls. Although PYD and work-to-failure are defined by several matrix compositional and organizational traits (Wang et al. 2001), the amount of mineral packed into the matrix (i.e., the mineral:matrix ratio) is particularly crucial because this trait is positively related to tissue stiffness but negatively related to tissue ductility (Currey 1984). Having higher TMDn may help compensate for smaller cross-sectional bone size by increasing the stiffness of the cortical tissue, but this comes at the expense of reduced ductility (decreased PYD) and reduced toughness (decreased work-to-failure). Consequently, the functional interactions between morphologic traits and tissue-quality traits creates preferred sets of traits for bone such that a wide bone (large TtAr) with low TMDn is preferred over a slender bone (small TtAr) with high TMDn.

Preferred sets of traits are not limited to the mouse skeleton; in fact, similar relationships between bone size and tissue-level mechanical properties have recently been reported for the human skeleton (Tommasini et al. 2005b, 2007). Young adult males and females with slender tibiae were found to have a compensatory increase in tissue-level stiffness and a concurrent reduction in tissue-level ductility and damageability when compared with individuals with

wider tibiae. The variation in tissue stiffness and ductility appeared to arise primarily from variation in ash content, similar to what we found for the mouse skeleton (unpublished data). This variation in tissue ductility may contribute to the increased incidence of stress fractures observed for young adult athletes (Crossley et al. 1999) and military recruits (Milgrom et al. 1989) having narrow bones. These studies suggest that functional interactions among morphologic and tissue-quality traits are similar for the mouse and human skeletons.

Female and male RI strains inherited bone traits in a similar manner

The similarity in *Z* scores between female and male RI strains indicated that males and females inherited bone traits in nearly identical manners. Our results differed from prior work that reported that whole-body BMD was inherited in a sex-specific manner for BXD RI strains (Orwoll et al. 2001). Further studies need to be conducted to resolve whether this discrepancy in sex-specific heritability is a function of the particular intercrosses (AXB/BXA versus BXD) or the nature of the traits that were examined (specific measures of morphology and tissue quality versus whole-body BMD). The path coefficients describing the functional interactions among bone size, cortical thickness, and tissue mineral density were similar for females and males, suggesting that sexual dimorphism did not appreciably affect the relationship among these traits. Furthermore, males and females showed similar path coefficients for the more complex models (Models B and C) indicating that both sexes showed similar relationships between mechanical properties and the underlying physical bone traits. This may help explain why none of the traits were inherited in a sex-specific manner.

Conclusions

The results of this study confirmed that a genetic randomization approach, which was originally developed for cardiovascular traits (Nadeau et al. 2003), can also be applied to bone to identify functional interactions among constituent traits. The path analysis provided evidence in support of our global hypothesis that organ-level functionality (i.e., stiffness, strength, toughness) was achieved through the coordinate regulation of multiple physical bone traits. In particular, the path analysis confirmed an important functional interaction between morphologic and tissue-quality traits. These interactions, which are likely fundamental to the adaptive process of bone, may explain why genetic variation in certain physical traits does not impair the ability of bone to function under day-to-day

activities. However, for certain genetic variations, this adaptive process creates a set of traits that would be expected to perform poorly under extreme loading conditions. These functional interactions may provide novel targets for genetic analyses. Given that functional interactions were critical for establishing whole-bone mechanical function, we expect that gene variants that perturb these interactions will also alter the repertoire of whole-bone mechanical properties. Identifying these variants will be important because certain alleles may lead to loss of function (i.e., more fragile bones), whereas others may lead to gain of function (i.e., more robust bones). Finally, the functional interaction between bone morphology and tissue quality has broader implications for clinical and genetic research in that knowledge of sets of traits, rather than a single trait, is needed to understand how pathologic conditions arise in the skeleton. Knowing the variable cellular activities that lead to preferred sets of adult traits may provide a new strategy for reducing fracture incidence throughout life.

Acknowledgment The authors thank the National Institutes of Health (AR44927, RR12305) for their support.

References

- Albright F, Smith PH, Richardson AM (1941) Post-menopausal osteoporosis. Its clinical features. *JAMA* 116:2465–2474
- Beamer WG, Shultz KL, Churchill GA, Frankel WN, Baylink DJ, et al. (1999) Quantitative trait loci for bone density in C57BL/6J and CAST/EiJ inbred mice. *Mamm Genome* 10:1043–1049
- Beck TJ, Ruff CB, Mourtada FA, Shaffer RA, Maxwell-Williams K, et al. (1996) Dual-energy X-ray absorptiometry derived structural geometry for stress fracture prediction in male U.S. Marine Corps recruits. *J Bone Miner Res* 11:645–653
- Beck TJ, Ruff CB, Shaffer RA, Betsinger K, Trone DW, et al. (2000) Stress fracture in military recruits: gender differences in muscle and bone susceptibility factors. *Bone* 27:437–444
- Bonadio J, Saunders TL, Tsai E, Goldstein SA, Morris-Wiman J, et al. (1990) Transgenic mouse model of the mild dominant form of osteogenesis imperfecta. *Proc Natl Acad Sci U S A* 87:7145–7149
- Bonadio J, Jepsen KJ, Mansoura MK, Jaenisch R, Kuhn JL, et al. (1993) A murine skeletal adaptation that significantly increases cortical bone mechanical properties. Implications for human skeletal fragility. *J Clin Invest* 92:1697–1705
- Chan GM, Hess M, Hollis J, Book LS (1984) Bone mineral status in childhood accidental fractures. *Am J Dis Child* 138:569–570
- Cheverud JM (1996) Developmental integration and the evolution of pleiotropy. *Am Zool* 36:44–50
- Churchill GA, Doerge RW (1994) Empirical threshold values for quantitative trait mapping. *Genetics* 138:963–971
- Crossley K, Bennell KL, Wrigley T, Oakes BW (1999) Ground reaction forces, bone characteristics, and tibial stress fracture in male runners. *Med Sci Sports Exerc* 31:1088–1093
- Cummings SR, Melton LJ (2002) Epidemiology and outcomes of osteoporotic fractures. *Lancet* 359:1761–1767
- Currey JD (1979) Mechanical properties of bone tissues with greatly differing functions. *J Biomech* 12:313–319

- Currey JD (1984) Effects of differences in mineralization on the mechanical properties of bone. *Philos Trans R Soc Lond B Biol Sci* 304:509–518
- Duan Y, Parfitt A, Seeman E (1999) Vertebral bone mass, size, and volumetric density in women with spinal fractures. *J Bone Miner Res* 14:1796–1802
- Duan Y, Seeman E, Turner CH (2001) The biomechanical basis of vertebral body fragility in men and women. *J Bone Miner Res* 16:2276–2283
- Ferretti JL, Capozza RF, Mondelo N, Zanchetta JR (1993) Interrelationships between densitometric, geometric, and mechanical properties of rat femora: inferences concerning mechanical regulation of bone modeling. *J Bone Miner Res* 8:1389–1396
- Frost HM (1987) Bone “mass” and the “mechanostat”: a proposal. *Anat Rec* 219:1–9
- Garn S (1970) *The earlier gain and the later loss of cortical bone* (Springfield, IL: Charles C. Thomas)
- Giladi M, Milgrom C, Simkin A, Stein M, Kashtan H, et al. (1987) Stress fractures and tibial bone width. A risk factor. *J Bone Joint Surg Br* 69:326–329
- Gilsanz V, Loro ML, Roe TF, Sayre J, Gilsanz R, et al. (1995) Vertebral size in elderly women with osteoporosis. Mechanical implications and relationship to fractures. *J Clin Invest* 95:2332–2337
- Grace JB (2006) *Structural Equation Modeling and Natural Systems* (Cambridge: Cambridge University Press)
- Jepsen KJ, Pennington DE, Lee YL, Warman M, Nadeau J (2001) Bone brittleness varies with genetic background in A/J and C57BL/6J inbred mice. *J Bone Miner Res* 16:1854–1862
- Jepsen KJ, Akkus OJ, Majeska RJ, Nadeau JH (2003) Hierarchical relationship between bone traits and mechanical properties in inbred mice. *Mamm Genome* 14:97–104
- Kiel DP, Hannan MT, Broe KE, Felson DT, Cupples LA (2001) Can metacarpal cortical area predict the occurrence of hip fracture in women and men over 3 decades of follow-up? Results from the Framingham Osteoporosis Study. *J Bone Miner Res* 16:2260–2266
- Klein RF, Mitchell SR, Phillips TJ, Belknap JK, Orwoll ES (1998) Quantitative trait loci affecting peak bone mineral density in mice. *J Bone Miner Res* 13:1648–1656
- Landin L, Nilsson BE (1983) Bone mineral content in children with fractures. *Clin Orthop Relat Res* 292–296
- Leamy L (1974) Heritability of osteometric traits in a randombred population of mice. *J Hered* 65:109–120
- Leamy LJ, Routman EJ, Cheverud JM (1999) Quantitative trait loci for early- and late-developing skull characters in mice: A test of the genetic independence model of morphological integration. *Am Naturalist* 153:201–214
- Li R, Tsaih S-W, Shockley K, Stylianou IM, Wergedal J, et al. (2006a) Structural model analysis of multiple quantitative traits. *PLoS Genet* 2:1046–1057
- Li W, Wang M, Irigoyen P, Gregersen PK (2006b) Inferring causal relationships among intermediate phenotypes and biomarkers: a case study of rheumatoid arthritis. *Bioinformatics* 22:1503–1507
- Li X, Masinde G, Gu W, Wergedal J, Hamilton-Ulland M, et al. (2002a) Chromosomal regions harboring genes for the work to femur failure in mice. *Funct Integr Genomics* 1:367–374
- Li X, Masinde G, Gu W, Wergedal J, Mohan S, et al. (2002b) Genetic dissection of femur breaking strength in a large population (MRL/MpJ x SJL/J) of F2 Mice: single QTL effects, epistasis, and pleiotropy. *Genomics* 79:734–740
- MacCallum RC, Hong S (1997) Power analysis in covariance structural modeling using GFI and AGFI. *Multivariate Behav Res* 32:193–210
- Martin RB, Ishida J (1989) The relative effects of collagen fiber orientation, porosity, density, and mineralization on bone strength. *J Biomech* 22:419–426
- Milgrom C, Giladi M, Stein M, Kashtan H, Margulies JY, et al. (1985) Stress fractures in military recruits. A prospective study showing an unusually high incidence. *J Bone Joint Surg Br* 67:732–735
- Milgrom C, Giladi M, Simkin A, Rand N, Kedem R, et al. (1989) The area moment of inertia of the tibia: a risk factor for stress fractures. *J Biomech* 22:1243–1248
- Mohan S, Masinde G, Li X, Baylink DJ (2003) Mapping quantitative trait loci that influence serum insulin-like growth factor binding protein-5 levels in F2 mice (MRL/MpJ x SJL/J). *Endocrinology* 144:3491–3496
- Nadeau JH, Burrage LC, Restivo J, Pao YH, Churchill G, et al. (2003) Pleiotropy, homeostasis, and functional networks based on assays of cardiovascular traits in genetically randomized populations. *Genome Res* 13:2082–2091
- Olson EC, Miller RL (1958) *Morphological Integration* (Chicago: The University of Chicago Press)
- Orwoll ES, Belknap JK, Klein RF (2001) Gender specificity in the genetic determinants of peak bone mass. *J Bone Miner Res* 16:1962–1971
- Otsu N (1979) A threshold selection method from gray-level histograms. *IEEE Trans Systems Man Cybern SMC-9*:62–66
- Price CP, Herman BC, Lufkin T, Goldman HM, Jepsen KJ (2005) Genetic variation in bone growth patterns defines adult mouse bone fragility. *J Bone Miner Res* 20:1983–1991
- Richman C, Kutilek S, Miyakoshi N, Srivastava AK, Beamer WG, et al. (2001) Postnatal and pubertal skeletal changes contribute predominantly to the differences in peak bone density between C3H/HeJ and C57BL/6J mice. *J Bone Miner Res* 16:386–397
- Stieger JH, Lind JM (1980) Statistically based tests for the number of common factors. Presented at the Annual Meeting of the Psychometric Society, Iowa City, IA
- Susanne C, Defrise-Gussenhoven E, Van Wansele P, Tassin A (1983) Genetic and environmental factors in head and face measurements of Belgian twins. *Acta Genet Med Gemellol (Roma)* 32:229–238
- Swartz SM, Bennett MB, Carrier DR (1992) Wing bone stresses in free flying bats and the evolution of skeletal design for flight. *Nature* 359:726–729
- Tommasini SM, Morgan TG, van der Meulen M, Jepsen KJ (2005a) Genetic variation in structure-function relationships for the inbred mouse lumbar vertebral body. *J Bone Miner Res* 20:817–827
- Tommasini SM, Nasser P, Schaffler MB, Jepsen KJ (2005b) Relationship between bone morphology and bone quality in male tibias: implications for stress fracture risk. *J Bone Miner Res* 20:1372–1380
- Tommasini SM, Nasser P, Jepsen KJ (2007) Sexual dimorphism affects tibia size and shape but not tissue-level mechanical properties. *Bone* 40:498–505
- Turner CH, Hsieh YF, Muller R, Bouxsein ML, Baylink DJ, et al. (2000) Genetic regulation of cortical and trabecular bone strength and microstructure in inbred strains of mice. *J Bone Miner Res* 15:1126–1131
- van der Meulen MC, Jepsen KJ, Mikic B (2001) Understanding bone strength: size isn't everything. *Bone* 29:101–104
- Wang X, Bank RA, TeKoppele JM, Agrawal CM (2001) The role of collagen in determining bone mechanical properties. *J Orthop Res* 19:1021–1026
- Wergedal JE, Sheng MH, Ackert-Bicknell CL, Beamer WG, Baylink DJ (2005) Genetic variation in femur extrinsic strength in 29 different inbred strains of mice is dependent on variations in

- femur cross-sectional geometry and bone density. *Bone* 36:111–122
- Wright S (1918) On the nature of size factors. *Genetics* 3:367–374
- Wright S (1921) Correlation and causation. *J Agric Res* 20:557–585
- Yershov Y, Baldini TH, Villagomez S, Young T, Martin ML, et al. (2001) Bone strength and related traits in HcB/Dem recombinant congenic mice. *J Bone Miner Res* 16:992–1003